Emergence of a Low-Viscosity Channel in the Northern Izu-Bonin Subduction System Through the Coupling of Mantle Flow and Thermodynamics and Implications for Melting in the Wedge

Laura Baker Hebert*, Paula Smith, Paul Asimow, and Michael Gurnis

California Institute of Technology; Pasadena, California, 91125

***labaker@gps.caltech.edu**

Abstract

We couple a petrological model (pHMELTS) with a 2D thermal and variable viscosity flow model (ConMan), to describe and compare fundamental processes occurring within subduction zones. We study the thermal state and phase equilibria of the subducting oceanic slab and adjacent mantle wedge and constrain fluid flux. Using a Lagrangian particle distribution to perform thousands of thermodynamically equilibrated calculations, the chemical composition of the domain is continuously updated.

Allowing the buoyancy and viscosity to be compositionally and thermally dependent permits a consistent linkage between the effect of water addition to and flow within the mantle wedge, leading to predictions as to the fate of the hydrated material as subduction proceeds. We present modeling results from the northern Izu-Bonin subduction system, involving subduction forcing functions such as convergence rate, slab dip, slab age, and upper plate thickness particular to that region. The coupling between the chemistry and the dynamics results in behavior previously unresolved, including the development of a continuous, slab-adjacent low-viscosity channel (LVC) defined by hydrous mineral stability and higher concentrations of water (up to thousands of ppm) in nominally anhydrous minerals (NAM).

The LVC develops due to fluid ingress into the mantle wedge from the dehydrating slab, and can be responsible for slab decoupling, large-scale changes in the wedge flow field, and a mechanism by which hydrated slab-adjacent wedge material can be transported to the deep mantle.

We observe multiple locations of fluid release along the subducting slab from dehydration reactions within eclogitic and serpentinized layers, leading to water weakening of mantle peridotite and a reduction in viscosity (10 to 100 times) in a region adjacent to the slab and resulting in an LVC on average 25 kilometers thick.

The limiting factor on the thickness of the LVC is due to the initiation of melting. The temperatures near the slab-wedge interface are too low for peridotite melting even under conditions of water-saturation. If a region is water-saturated, fluid will continue to move vertically into the wedge and is bound further from the slab into progressively hotter areas. Eventually the hydrated solidus is crossed and melting begins. This forms an upper boundary to the hydrated low-viscosity region, controlling the channel geometry. A closer examination of the melting region shows a progressively increasing slab-normal distance of melt initiation into the wedge (thickening LVC) with depth due to depletion of mantle material by melting at shallower depths. Assuming a near-fractional melting scheme, the melting region is quite localized to an area immediately above the LVC. We compare variations in primary lava compositions in the Izu-Bonin subduction system to the range of hydrous melts derived from the upper surface of the LVC in our models.

Conclusions

(1) Slab thermal age and convergence angle play important roles in determining fluid release locations and the structure of the LVC

(2) The LVC provides a potential first-stage of rapid transport in a two-stage water migration scheme

(3) Formation of the LVC has both geophysical and geochemical implications

(4) Melting is spatially restricted, bounded by the top of the LVC (water-saturated solidus) and by water activity dropping below 1.0 due to partitioning in the melt phase

(5) The spatial separation of fluid sources provides for a range of primary melt compositions

(6) Progressive depletion of the mantle source leads to an angling of the melt source region away from the slab into the wedge interior

(7) Cooling of the wedge over time can lead to dramatic changes in the locations of melt production and the path length of fluid transport

Motivation

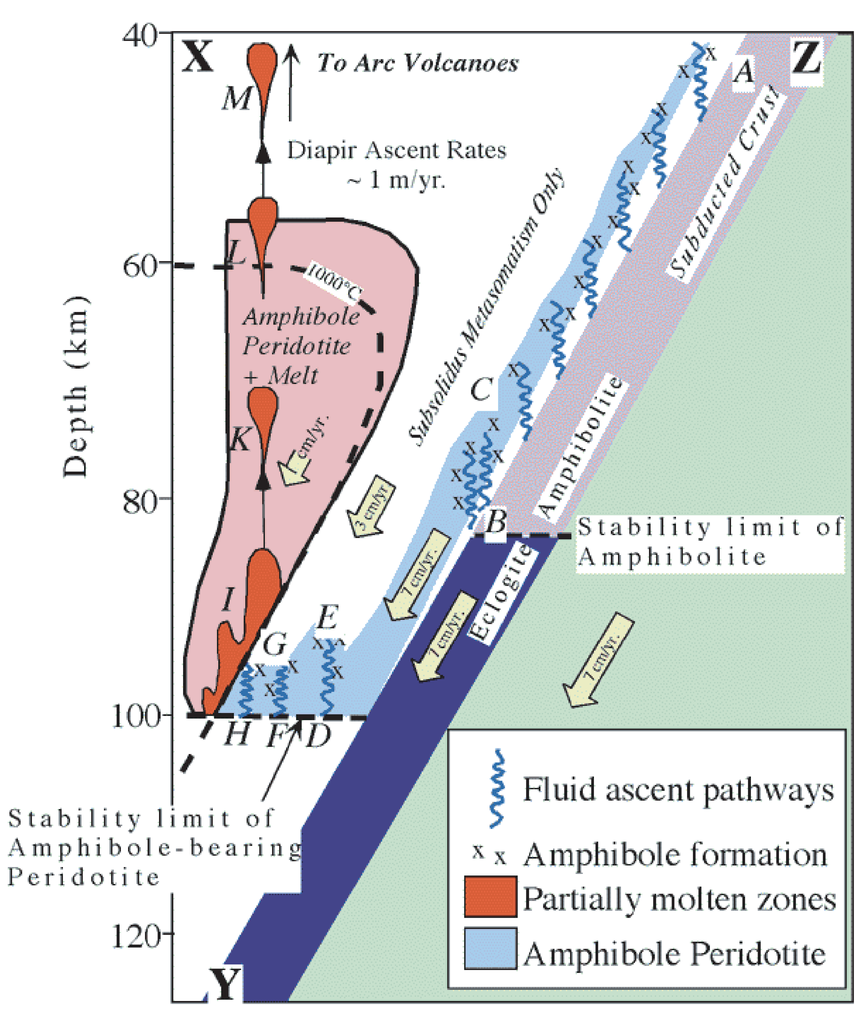

Figure from R.Stern; adapted from Davies and Stevenson (1992)

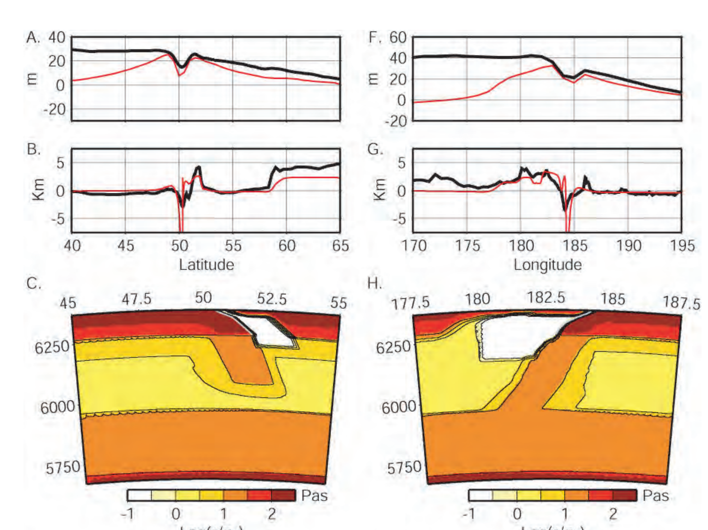

Figure from Billen and Gurnis (2003)

Many aspects of subduction zone science have yet to be fully understood; including where fluid is released from the slab, how much water is deeply subducted, how fluid transits the wedge, the role of the hydration of NAM on the fluid budget and on the rheology, and where melting initiates.

We will investigate these aspects in the context of a fully-coupled geodynamic and geochemical model, allowing the chemistry to influence the dynamics, and vice versa.

Development of the LVC

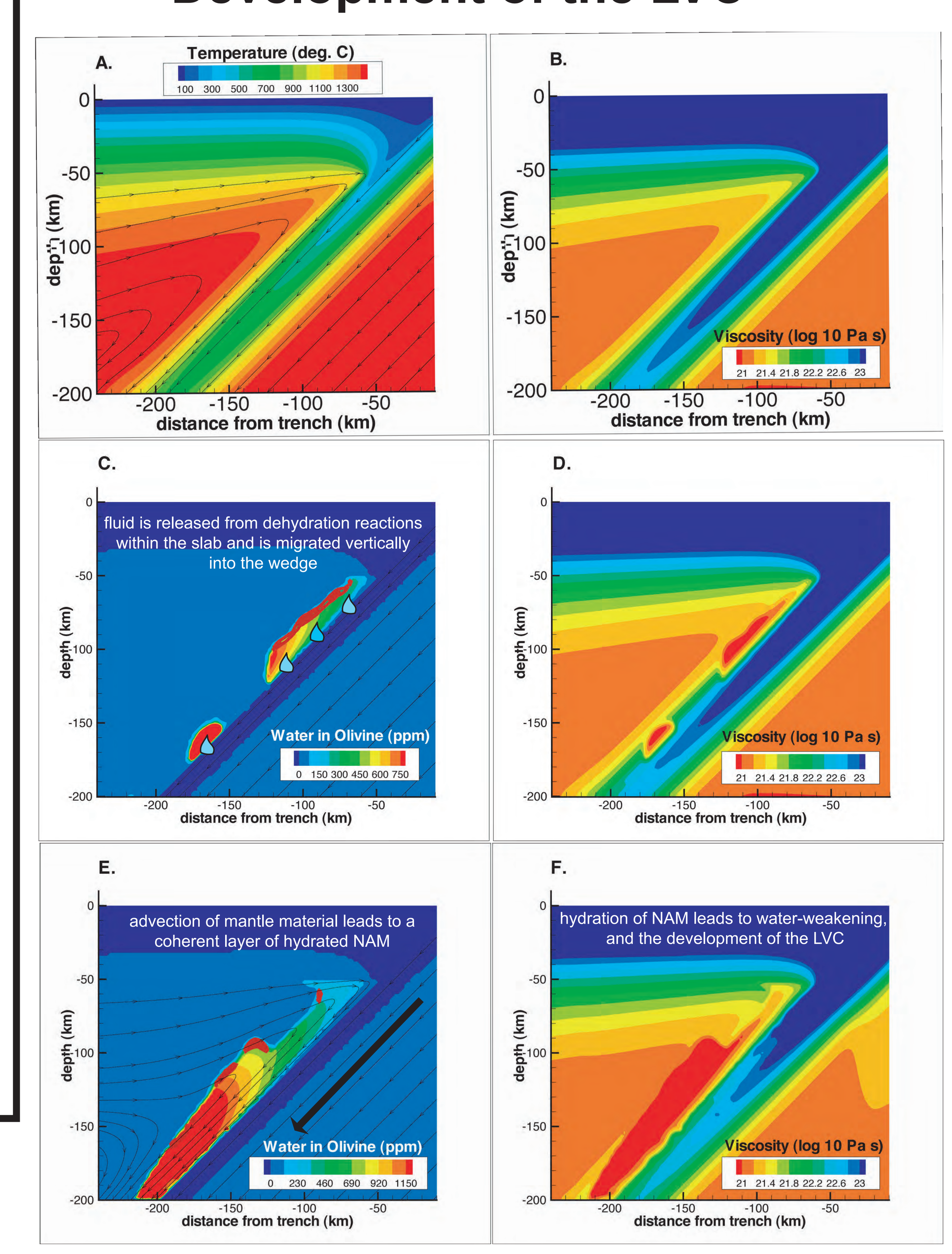

Controls on the Shape of the LVC

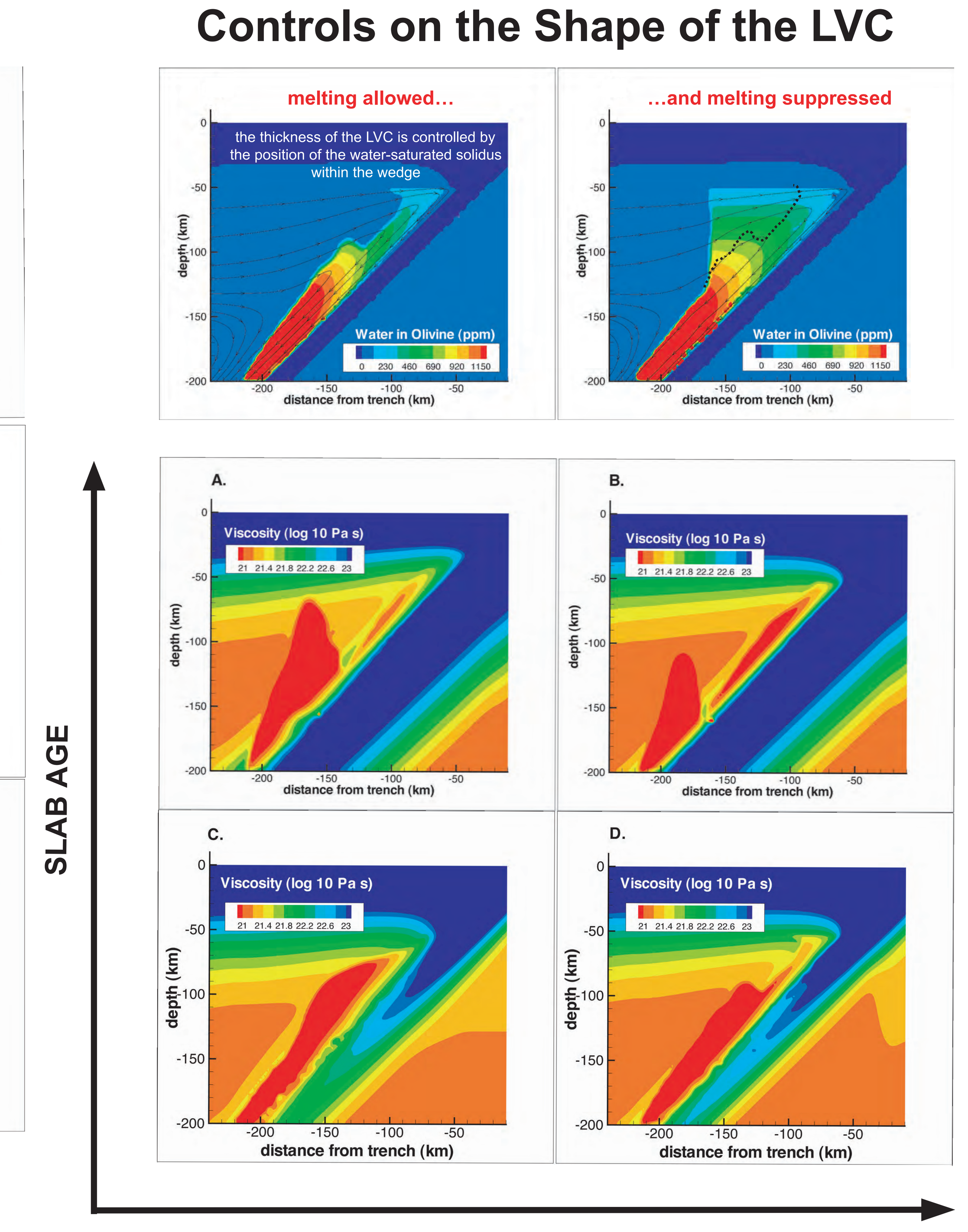

DECREASING SLAB DIP ANGLE

INCREASING SLAB DIP ANGLE

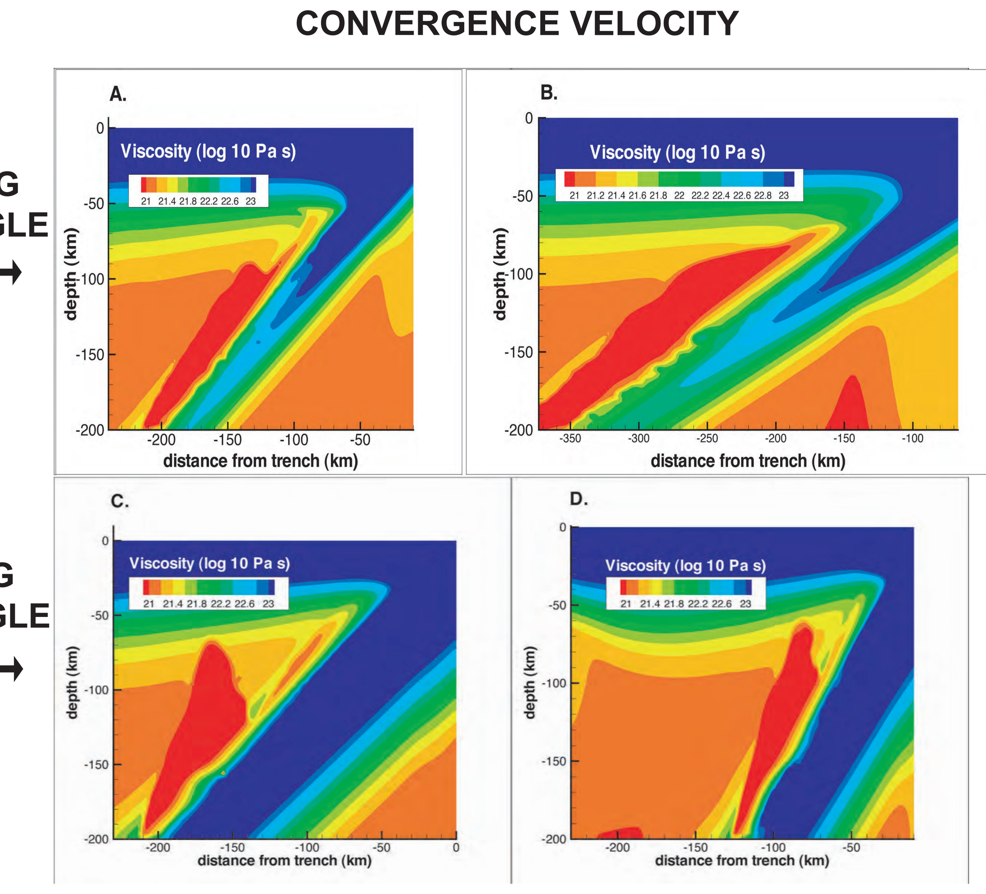

Model Set-up

full coupling between two separate models using parallel computing:

(1) ConMan: 2D thermal and variable viscosity numerical flow model

$$\frac{\partial S}{\partial t} = -v \cdot \nabla S + \left(\frac{C_p}{S_0}\right)\frac{\nabla^2 T}{T}$$

$$\eta' = \frac{\eta}{\eta_0} = \exp\left[\frac{Q}{RT_0} * \left(\frac{T_0}{T} - 1\right)\right] * \left[\frac{XH2O_{ij}}{XH2O\_crit}\right]^{-1}$$

(2) pHMELTS: thermodynamic energy minimization algorithm that can calculate water partitioning in nominally-anhydrous minerals (NAM) in addition to hydrous phases, melt, and vapor

GyPSM-S:

Geodynamic and **P**etrological **S**ynthesis **M**odel for **S**ubduction

Subduction parameter space includes variations in slab dip, slab thermal age, convergence velocity, and over-riding plate thickness

Wedge calculations are solved by pHMELTS, with alternate solvers employed to handle conditions outside the pHMELTS realm of stability
- Olivine solubility measurements from Mosenfelder et al. (2006)
- DMM mantle initial composition from Workman and Hart (2005), with 110 ppm H2O bulk

Slab dehydration reactions governed by Hacker et al. (2003) phase diagrams
- The hydration depth into the slab consists of a 7-km thick altered oceanic crustal layer, and a 5-km thick serpentinite layer

The top surface is isothermal (273 K), and the thickness of the over-riding plate and thermal age of the down-going slab determine the initial thermal conditions

The slab velocities are kinematically imposed, with an analytical corner-flow solution (Batchelor, 1967) along the left boundary

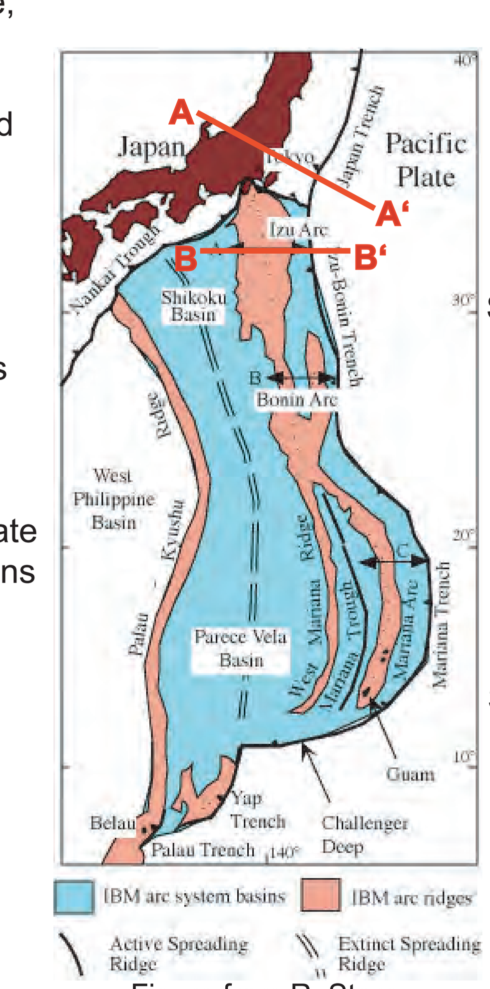

Figure from R. Stern

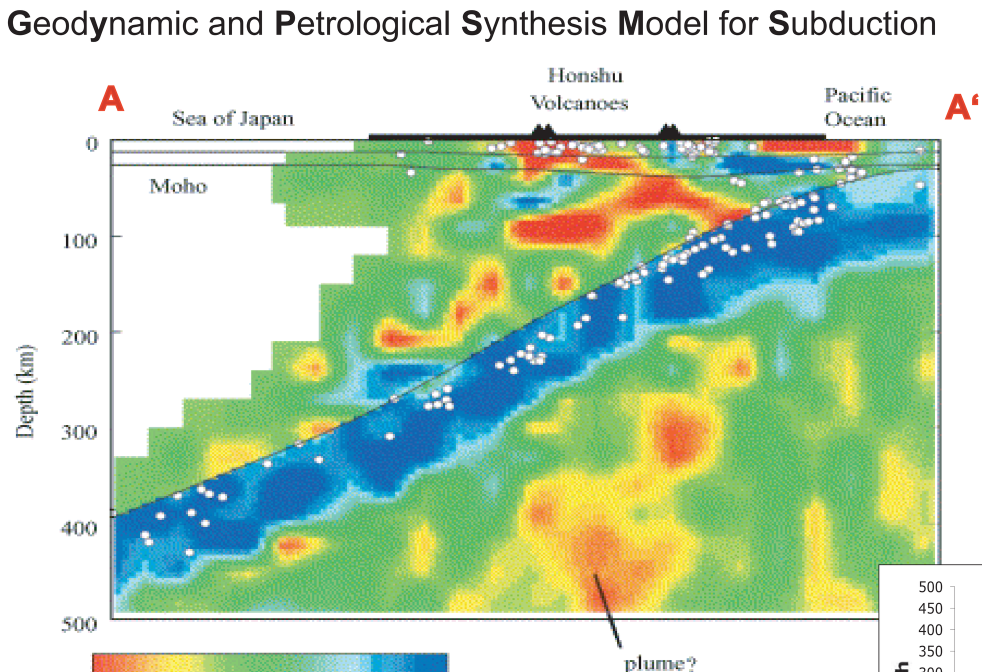

Figure from Zhao (2004)

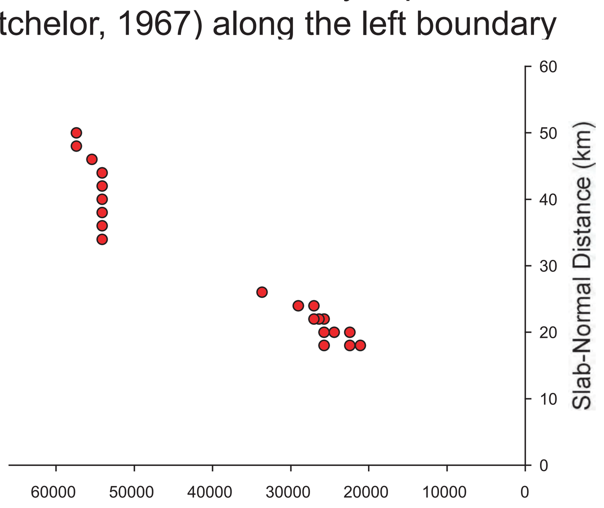

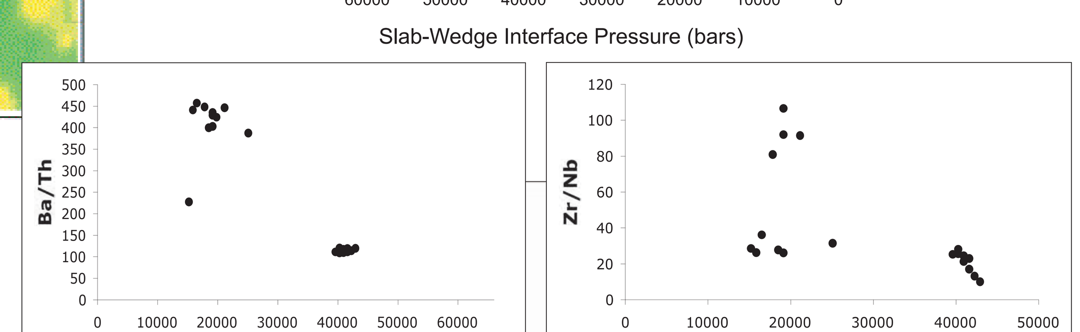

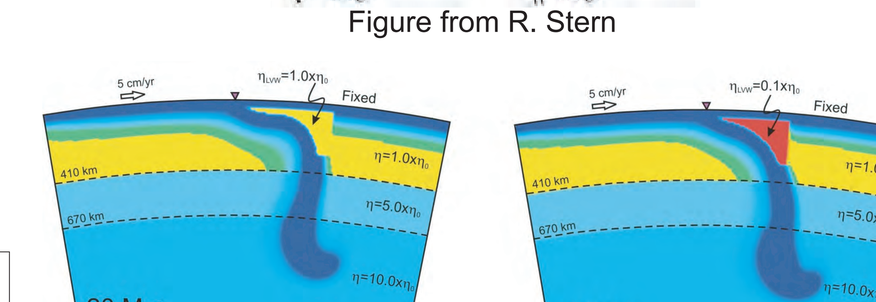

Figure from Manea and Gurnis (2007)

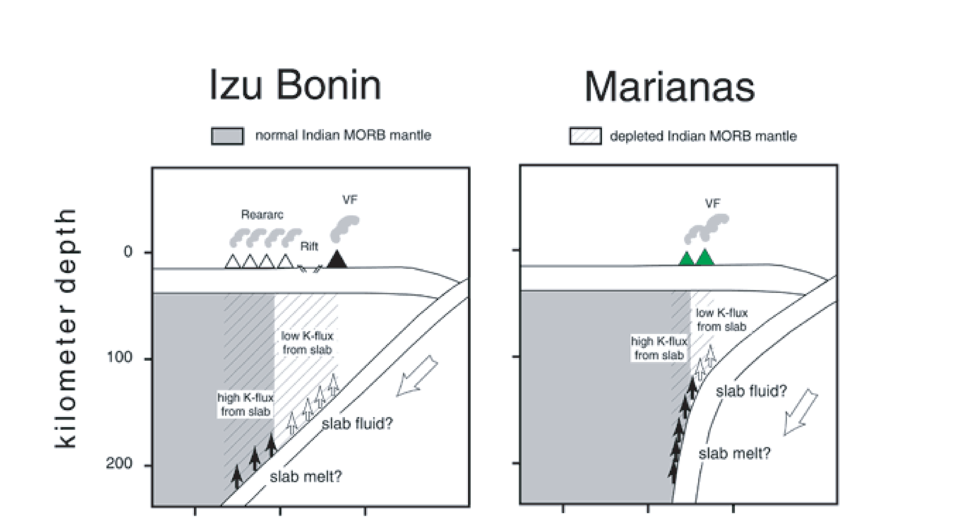

Figure from Straub (2003)

The melting region of the evolved Northern Izu-Bonin subduction zone involves a shallowing of the deeper melting sources through wedge cooling, allowing fluids to reach into the wedge corner.

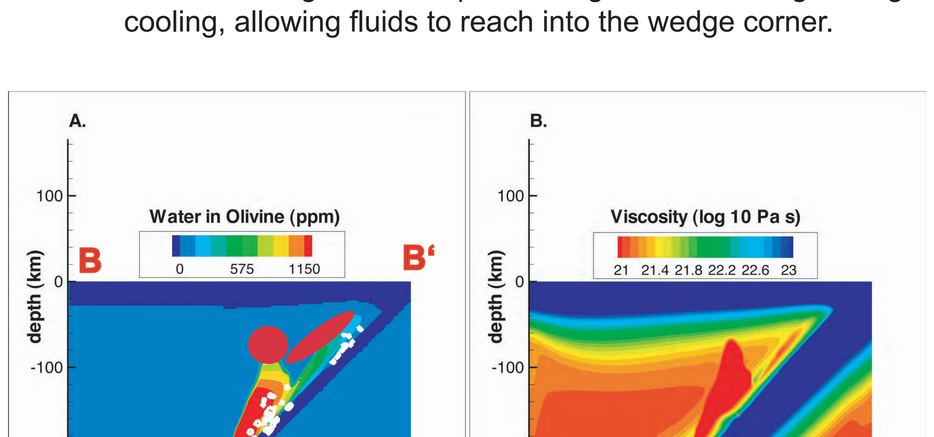

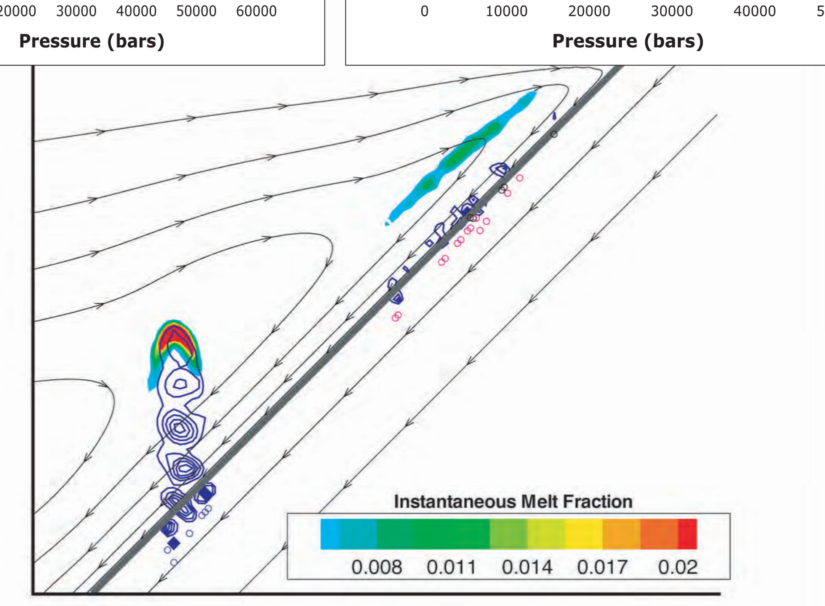

Melting initiates immediately above fluid release locations, above the saturated LV-zone

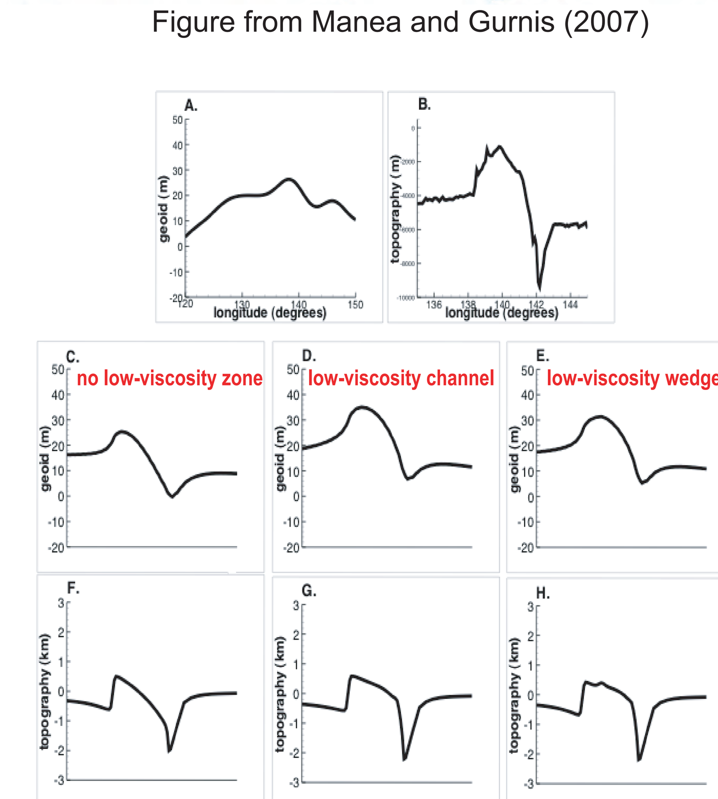

Hirth and Kohlstedt (1996) Earth and Planetary Science Letters 144 (1-2), 93-108.
Billen and Gurnis (2001) Earth and Planetary Science Letters 193, 227-236.
Billen and Gurnis (2003) G^3 4(4).
Smith and Asimow (2005) G^3 6(2).
Ghiorso and Sack (1995) Contributions to Mineralogy and Petrology 119 (2-3), 197-212.
King et al. (1990) Physics of the Earth and Planetary Interiors 59 (3), 195-207.
Batchelor (1967) An Introduction to Fluid Dynamics, Cambridge University Press.
Ghiorso et al. (2002) G^3 3.
Berman (1988) Journal of Petrology 89, 168-183.
Mosenfelder et al. (2006) American Mineralogist 91(2), 285-294.
Workman and Hart (2005) Earth and Planetary Science Letters 231(1-2), 53-72.
Hacker et al. (2003) Journal of Geophysical Research-Solid Earth 108 (B1).
Stern et al. (An Overview of the Izu-Bonin-Mariana Subduction Factory. Geophysical Monograph 138, 175-222.
Manea and Gurnis (2007) Earth and Planetary Science Letters.
Davies and Stevenson (1991) Journal of Geophysical Research 97(B2), 2037-2070.
Straub (2003) G^3 4(2).
Zhao (2004) Physics of the Earth and Planetary Interiors 146, 3-34.